ISSN 1729–5106

EAST AFRICAN JOURNAL OF PHYSICAL SCIENCES

Volume 6 — Part 1 July 2005

Contents

An International Journal of Pure and Applied Science

East African Journal of Physical Sciences 6(1): 21–31 (2005)

The use of mesh generation function for the solution of natural convection problems

Francis K. Gatheri
Mathematics Department, Kenyatta University, P.O. Box 43844 - 00100, Nairobi, Kenya.
kgatheri@avu.org

A mesh generation procedure for the solution of coupled, non-linear, partial differential equation is described. The essence of the procedure is the use of a grid generating function, which results in a strong refinement along the walls.

In viscous fluid flow, the problem arises where the solution varies rapidly over a small part of the domain but over the rest of the domain changes very slowly. At very large Reynolds number, viscous fluid flow pattern changes rapidly in narrow boundary layers close to walls where the fluid is brought to rest. In such convection dominated flows it is desirable to concentrate more mesh points in certain regions of the cavity. This is in order to place more mesh points within areas of steep velocity gradients.

The effectiveness of the procedure is demonstrated by applying it to the problem of turbulent natural convection in an enclosure with colliding boundary layers.

Key words: grid generator, natural convection, and turbulent flows.

INTRODUCTION

In most studies of rectangular enclosures two types of meshes are used, uniform mesh and non-uniform (stretched) mesh. A uniform mesh involves subdividing the rectangular cavity in Figure1 into uniform rectangular volume elements which represents volumes centred about mesh points, whose coordinates are denoted by integer variables i, j, k where $x=(i-1)h_x$, $y=(j-1)h_y$, $z=(k-1)h_z$, $h_x=ARX/M-1$, $h_y=ARY/N-1$ and $h_z=ARZ/L-1$, $1<i<M$, $1<j<N$, $1<k<L$. ARX, ARY and ARZ are the aspect ratios in the x, y and z directions respectively and M, N and L are the total numbers of nodes in the x-,y- and z-direction respectively. It should be noted that there are mesh points on the boundaries of the solution region. This is a common approach where the stream function/vorticity formulation is used and extended to the vorticity/vector-potential formulation (Mallison, 1974).

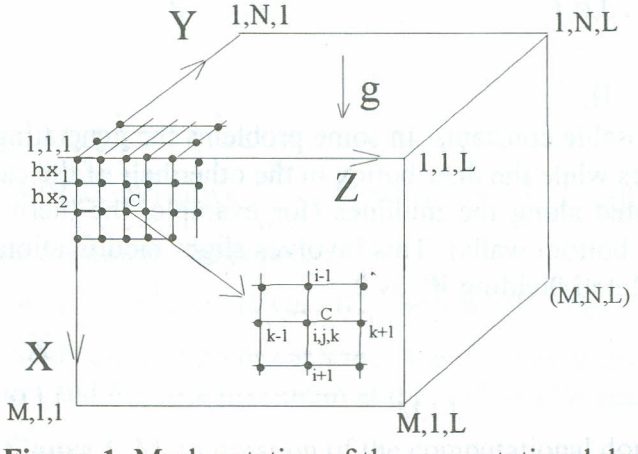

Figure 1. Mesh notation of the computational domain.

In viscous fluid flow, the problem arises where the solution varies rapidly over a small part of the domain but the rest of the domain changes very slowly. At very large Reynolds numbers, viscous fluid flow pattern changes rapidly in narrow boundary layers close to walls where the fluid is brought to rest. In some cases, for example turbulent shear driven flow, it is possible to derive asymptotic expansions applicable in the boundary layers, which can be matched smoothly to numerical or analytic solution in the interior (Jones & Thompson, 1980). However, this is usually not possible and the boundary layer has to be resolved numerically by ensuring that several mesh point's fall within them.

In some problems, in particular convection dominated ones, it is desirable to concentrate more mesh points in certain regions of the cavity. This is in order to place more points within areas of steep velocity gradients. This can be accomplished by assigning spatially varying values of h_x, h_y *and* h_z in the formulation of the finite difference equation (Thomas, 1970). Alternatively, the independent space variables may be transformed and the resulting equation solved in terms of the new variables using a uniform mesh (Newel & Schmidt, 1970).

The calculation of first and second derivatives by applying central differences on a uniform grid gives approximation, which is second order $0(h^2)$ accurate in the mesh interval. However, if a non-uniform grid is used, truncation error analysis can be used to demonstrate that one order of accuracy is lost in the case of the second derivative, the difference approximation becoming first order only (Gatheri, 1994). In order to maintain second order accuracy a uniform grid with an extremely fine mesh may be used to obtain a sufficient number of points in the boundary layers. The increase in the size of the problem may make the computation prohibitively expensive.

MESH GENERATOR

This technique of grid generation, make use of a grid generating function, which results in strong grid refinement along the walls. The generating function, generates grid points for the full cavity. The mesh points, say in the x-direction, are positioned according to

$$x_i = W_o\left(1+\alpha\left(\frac{i-1}{M-1}\right)^p\right)(i-1) \tag{1}$$

where

$$W_o = ((1+\alpha)(M-1))^{-1} \tag{2}$$

α and p are disposable constants. In some problems the generating function, generates only half the total grid points while the distribution in the other half of the cavity is set so that they are symmetrically distributed along the midlines (for example, the thermally driven square cavity with adiabatic top and bottom walls). This involves slight modification of equations (1) and (2), replacing M with $M/2$ and dividing W_o by 2.

NEAR-WALL MESH SPACING

We consider, for the sake of discussion the x-direction only. For i = 1,2,3....M. Using equation (1) and defining

$$h_x(i) = x(i) - x(i-1)$$

$$= W_o + \frac{\alpha W_o}{(M-1)^p}\left\{(M-1)^{p+1} - (M-2)^{p+1}\right\} \tag{3}$$

Therefore for $i<M$ the near wall grid spacing is close to

$$h_x(i) \approx W_o = \frac{1}{(1+\alpha)(M-1)} \tag{4}$$

Thus $(1+\alpha)^{-1}$ times more resolution in near wall regions is obtained compared with a uniformly spaced grid, which should be

$$h_x(i) = \frac{1}{(M-1)} \tag{5}$$

In this method it is possible to determine *apriori* the resolution near the wall depending on the choice of α, for a given number of grid points. This is not the case with the commonly used mesh generation in the literature, where the grid must be first generated before the near-wall resolution can be checked near the wall.

MESH EXPANSION RATIOS THROUGHOUT THE CAVITY

Locally uniform spacing, as well as a high density of grid points, is necessary if accurate solutions in the boundary layer are to be obtained. In this scheme increasing the exponent p has the effect of lowering the mesh expansion ratio near the wall $(R(i) = h_x(i+1)/h_x(i) \to 1)$ and increasing the expansion interval further into the flow interior. Care is also taken to ensure that second order accuracy is maintained throughout the flow region. This is shown in the following:

$$R(i) = \frac{h_x(i+1)}{h_x(i)}$$

$$= \frac{1+\beta\left(i^{p+1} - (i-1)^{p+1}\right)}{1+\beta\left((i-1)^{p+1} - (i-2)^{p+1}\right)} \tag{6}$$

where

$$\beta = \frac{\alpha}{(M-1)^p}$$

For a local maximum, the derivative $\frac{dR}{dm} = 0$, where $m = i-1$. After some mathematical manipulation, the following condition is obtained

$$0 = (m+1)^p - 2m^p + (m-1)^p + \beta\left\{2(m-1)^p(m+1)^p - m^p\left[(m-1)^p + (m+1)^p\right]\right\} \tag{7}$$

the solution of (7) would yields the grid point i at which the mesh expansion ratio is a maximum. If p=1, there is no maximum and $R(i)$ is a maximum at the wall and decreases monotonically into the cavity interior (Figure 2).

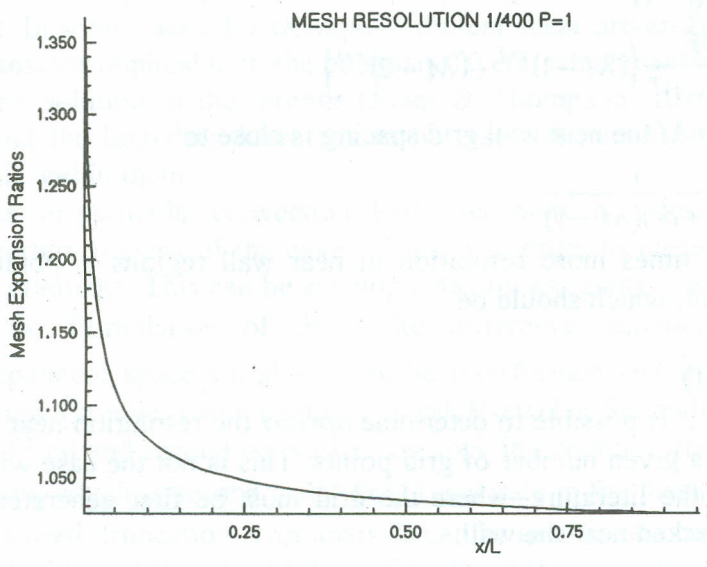

Figure 2. Mesh expansion ratios across the cavity for a 41 nodal grid, $\alpha = 9$, $p = 1$.

Substituting $p = 2$ in equation (7) and simplifying yields

$$m = \left(\frac{1+\beta}{3\beta}\right)^{1/2} \tag{8}$$

so that if, say $\alpha = 9$ and a 21 by 21 by 21 grid is used, near wall resolution is equivalent to 1/200, that is, a 201 by 201 by 201 grid, while the maximum mesh expansion ratio occurs at $i = m+1 \approx 5$ and $R_{max} = R(5) \approx 1.29$. The value of R_{max} is slightly high, and at least 3 points are needed between the wall and the velocity maximum (Quon, 1983).

For a 41 by 41 by 41 grid and for the same near wall resolution of 1/200 would require to set $\alpha = 4$ and R_{max} would occur at $i = m+1 \approx 13$ and $R_{max} = R(13) \approx 1.09$. Assuming the boundary layer thickness is approximately 0.02, that is, 4 points between the wall and velocity maximal, the grid point at which R_{max} occur will be in the flow interior, while also the value of R_{max} is very low. Therefore, the chosen mesh point should not introduce any significant discretization error due to non-uniformity.

For p>3, an approximation solution for m is given by

$$m = \left(\frac{p-1}{\beta(p+1)}\right)^{1/p} \tag{9}$$

for which

$$i_{R\max} = m+1 = \left(\frac{p-1}{\alpha(p+1)}\right)^{1/p}(M-1)+1 \tag{10}$$

Increasing the exponent p has the effect of increasing the number of nodes away from the wall at which R_{max} occurs until, in the limit $p \to \infty^+$, R_{max} occurs at the last node i_c. In most applications used in this paper, $p>5$ is rarely used.

In this method it is possible to get a very fine near-wall resolution, with a least five approximately uniformly spaced nodes ($p \leq 5$) and low R_{max} (≤ 1.5). Figure 3 shows that the use of more grid points results in more uniformly spaced nodes near the wall and lower R_{max}.

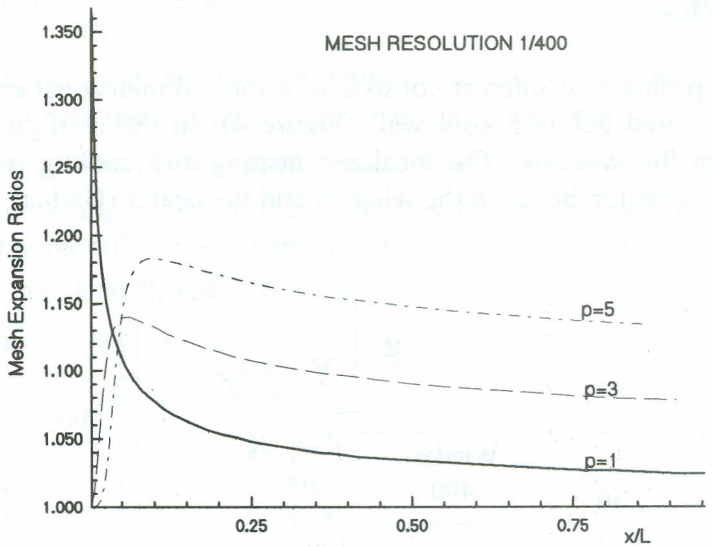

(a)

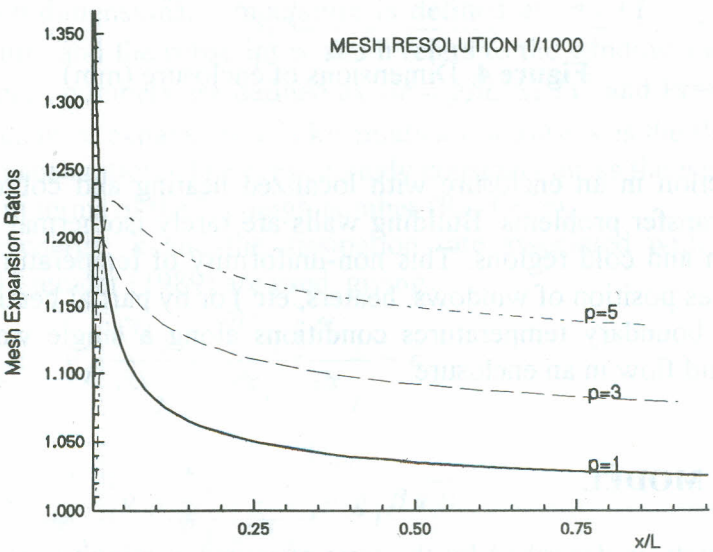

(b)

Figure 3. Mesh expansion ratios across the cavity for a 41 nodal grid (a) $\alpha = 9$, for $p = 1,3,5$ (b) $\alpha = 24$, for $p = 1, 3, 5$.

It should be noted that if a very fine near wall resolution is needed, it is not possible to maintain second order accuracy in the solution procedure. Consequently the first, say, 10-mesh point are kept uniform equivalent to the near wall grid spacing. The rest of the mesh points are positioned according to equation (1).

TURBULENT NATURAL CONVECTION IN AN ENCLOSURE WITH COLLIDING BOUNDARY LAYERS

The geometry of the problem of interest consists of a three-dimensional enclosure containing a convection heater mounted below a cold wall (Figure 4). In the configuration considered the heater is smaller than the window. The localized heating and cooling induces two boundary layers that collide in the region between the window and the heater (Gatheri, 1994).

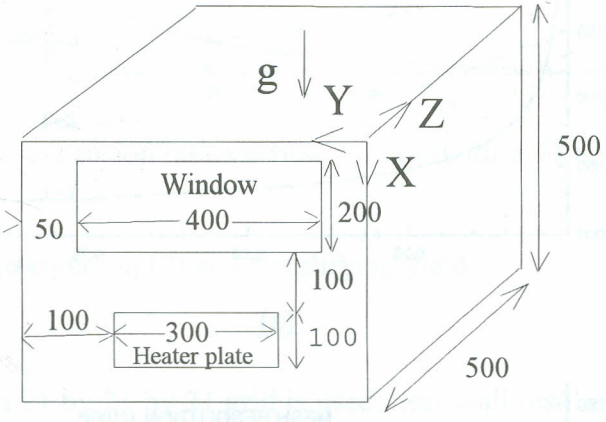

Figure 4. Dimensions of enclosure (mm).

Natural Convection in an enclosure with localized heating and colliding is relevant to a wide range of heat transfer problems. Building walls are rarely isothermal and more often than not, they poses warm and cold regions. This non-uniformity of temperature may be a result of building fabric (such as position of windows, heaters, etc.) or by partial heating of the wall by the sun. These different boundary temperatures conditions along a single wall may significantly affect the heat and fluid flow in an enclosure.

MATHEMATICAL MODEL

The motion in the cavity is described by the time averaged continuity, momentum and energy equations. Since the temperature difference between the heater and the window are below 50°C, the Bousinesq approximation is invoked. This means that all the transport properties are assumed to be constant except for the density in the buoyancy term of the momentum equation. The equations governing natural convection within the cavity are presented below in non-dimensional form for an incompressible, turbulent flow.

$$\frac{\partial U_i}{\partial x_i} = 0 \tag{11}$$

$$\frac{\partial U_i}{\partial t} + \frac{\partial}{\partial x_j}\left(U_j U_i\right) = -\frac{\partial P}{\partial x_i} + \frac{1}{\sqrt{Gr}}\nabla^2 U_i - \frac{\partial}{\partial x_j}\left(\overline{u_i u_j}\right) - \Theta g_i \tag{12}$$

$$\frac{\partial \theta}{\partial t} + \frac{\partial}{\partial x_j}\left(U_j \Theta\right) = \frac{1}{\Pr\sqrt{Gr}}\nabla^2 \Theta - \frac{\partial}{\partial x_j}\left(\overline{u_j \theta}\right) \tag{13}$$

In the above, upper and lower case letters refer to mean and fluctuating quantities respectively, U_i, P and Θ are the non-dimensional velocity, pressure and temperature respectively and g_i is the direction cosine of the gravitational vector with the x_i direction. The Reynolds stresses and heat fluxes are obtained from the low-Reynolds-number k-ε model (Jones & Launder, 1972) with the modified coefficients recommended by Launder and Sharma (1974). The turbulent stresses $\overline{u_i u_j}$ and heat fluxes $\overline{u_j \theta}$ are given by

$$\overline{u_i u_j} = -\nu_t\left(\frac{\partial U_i}{\partial x_j} + \frac{\partial U_j}{\partial x_i}\right) - \frac{2}{3}k\delta_{ij} \tag{14}$$

$$\overline{u_j \theta} = -\frac{\nu_t}{\delta_T}\frac{\partial \Theta}{\partial x_j} \tag{15}$$

All quantities in equation (11) to (15) were non-dimensionalized using the convection velocity, $U_c = \sqrt{g\beta\Delta T L}$, the reference length L, and here taken as the size of the enclosure in the z-direction. Θ the non-dimensional temperature is defined as $\Theta = (T - T_w)/(T_h - T_w)$. T is the dimensional temperature and the subscript w and h refers to the window and heater respectively. The Grashof and Prandtl numbers are defined as $Gr = g\beta L^3 \Delta T / \nu^2$ and Pr=ν/α respectively; β is the volumetric coefficient of expansion, ν is kinematics viscosity, κ is the thermal diffusivity and g is the gravitational acceleration. The present study considers air as the working fluid (Pr=0.71) and results are given in terms of the Rayleigh number (Ra=GrPr).

The turbulence energy, k and the dissipation rate associated with spectral transfer, $\tilde{\varepsilon}$, proposed by Ince and Launder (1989) are used, giving

$$\frac{\partial k}{\partial t} + \frac{\partial}{\partial x_j}U_j k = \nu_t\left(\frac{\partial U_i}{\partial x_j} + \frac{\partial U_j}{\partial x_i}\right)\frac{\partial U_i}{\partial x_j} - \tilde{\varepsilon}$$

$$- 2\nu\left(\frac{\partial k^{1/2}}{\partial x_j}\right)^2 + \frac{\partial}{\partial x_j}\left[\left(\nu + \frac{\nu_t}{\delta_k}\right)\frac{\partial k}{\partial x_j}\right] - g_i \beta \overline{u_i \theta} \tag{16}$$

$$\frac{\partial \tilde{\varepsilon}}{\partial t} + \frac{\partial}{\partial x_j} U_j \tilde{\varepsilon} = C_{\varepsilon 1} \frac{\tilde{\varepsilon}}{k} \nu_t \left(\frac{\partial U_i}{\partial x_j} + \frac{\partial U_j}{\partial x_i} \right) \frac{\partial U_i}{\partial x_j}$$
$$- C_{\varepsilon 2} \frac{\tilde{\varepsilon}^2}{k} + 2\nu\nu_t \left(\frac{\partial^2 U_i}{\partial x_j \partial x_k} \right)^2 + \frac{\partial}{\partial x_j} \left[\left(\nu + \frac{\nu_t}{\delta_\varepsilon} \right) \frac{\partial \tilde{\varepsilon}}{\partial x_j} \right] \tag{17}$$
$$+ 0.83 \left(\frac{k^{3/2}}{\tilde{\varepsilon} C_1 y} - 1 \right) \left(\frac{k^{3/2}}{\tilde{\varepsilon} C_1 y} \right)^2 \frac{\tilde{\varepsilon}^2}{k} - g_i \beta \overline{u_i \theta} \frac{\tilde{\varepsilon}}{k}$$

In this model the eddy viscosity ν_t is calculated from $\nu_t = c_\mu k^2 / \tilde{\varepsilon}$.

Here we take the generalized gradient diffusion hypothesis first introduced by Daly and Harlow (1970) leading to

$$\overline{u_j \theta} = -\frac{k}{\varepsilon} \overline{u_i u_k} \frac{\partial \Theta}{\partial x_k} \tag{18}$$

where $C_\theta = 1.5 c_\mu / \delta_T$, $\varepsilon = \tilde{\varepsilon} + 2\nu \left(\partial k^{1/2} / \partial x_k \right)^2$ and $\overline{u_i u_k}$ is given by equation (4). The following coefficients are adopted from Launder and Sharma (1974).

$c_\mu = 0.09 \exp\left(-(3.4/(1 + R_t/50)^2) \right)$ $\qquad$ $C_{\varepsilon 2} = 1.92 \left(1 - 0.3 \exp\left(-R_t^2 \right) \right)$

$R_t = k^2 / \nu\tilde{\varepsilon}$, $C_{\varepsilon 1} = 1.44$, $\qquad$ $\delta_\theta = 0.9, \delta_k = 1.0, \delta_\varepsilon = 1.3$

The problem associated with the use of primitive variables, namely, the pressure and the requirement of solving the continuity equation is overcome by recasting the momentum equation in a vorticity-vector potential formulation (Mallison & de Vahl Davis, 1977). The vorticity $\bar{\zeta}$ is defined as $\bar{\zeta} = \nabla \times U$, so that, by taking the curl of the momentum equation (12) and rearranging results in the vorticity transport equation.

If the vector potential, $\bar{\psi}$, is defined by $U = \nabla \times \bar{\psi}$ and is presumed to be solenoidal ($\nabla . \bar{\psi} = 0$), $\bar{\psi}$ is related to the vorticity by

$$\bar{\zeta} = \nabla \times U = -\nabla^2 \bar{\psi} \tag{19}$$

The walls of the enclosure are impermeable and stationary resulting in zero values for both the normal and tangential component of velocities. The boundary conditions for the vector potential derived by Hirasaki and Hellums (1968) are used in the study, i.e. $\partial \psi_n / \partial n = \psi_{t1} = \psi_{t2} = 0$ in which n refers to the direction normal to a wall and *t1* and *t2* refer to directions in the plane of a wall.

The vorticity boundary conditions were derived from equation (19) as outlined by Mallision and de Vahl Davis (1977).

The temperature is zero on the window and unity on the heater. On other parts of the walls, and on the floor and ceiling, we have assumed that $\partial \Theta / \partial n = 0$.

The turbulent kinetic energy k and the rate of dissipation of turbulent kinetic energy ε were set to zero on all the walls.

RESULTS AND DISCUSSION

A 41 by 41 by 41 non-uniform mesh was used as shown in Figure 5. A non-uniform grid distribution was employed in the axis perpendicular to the heater and window in order to have

sufficient nodal points placed between the wall and the position at which the velocity maximum occurred, and also to try to resolve the fine vortical structure observed in the experiment by both Humphrey and Bleinc (1985) and Cooper and Kulkarni (1993). The grid in the z-direction are positioned according to the grid generating techniques described above. The stretching in the z-direction was obtained by applying $\alpha = 19$ and $p = 5$.

In this method it is possible to get a very fine near wall resolution, with at least five approximately uniformly spaced nodes.

In the confluence region of the colliding boundary layers, there is significant heat transfer evident by the high temperature gradients. The localized heating and cooling along the vertical wall induces two boundary layers that collide in the region between the window and the heater. Along the active wall (Figure 6) two opposed boundary layers develop and move towards each other. The two boundary layers collide in the region between the heater and the window. As shown in Figures 6 (a) and (b) the hot stream initially moves parallel to the vertical wall. After collision the two boundary layers curve to form a short horizontal jet that moves into the enclosure. This stream then curved upwards spreading in the upper region as it moves toward the ceiling. The flow impinges on the ceiling and spreads on it. The flow returns to the active wall near the ceiling and floor of the cavity. A slow counterclockwise cell is formed in the upper half of the enclosure between the upwards moving stream and the cold downwards draught from the window.

The flow is similar to those observed in the experimental results of Sanjurjo and Cooper (1991) and Cooper and Kulkarni (1993) and the numerical results reported by de Vahl Davis *et al.* (1988). The horizontal temperature gradients generates vorticity that drives the flow. The cold downwards fluid from the window is congregated towards the lower edge of the window.

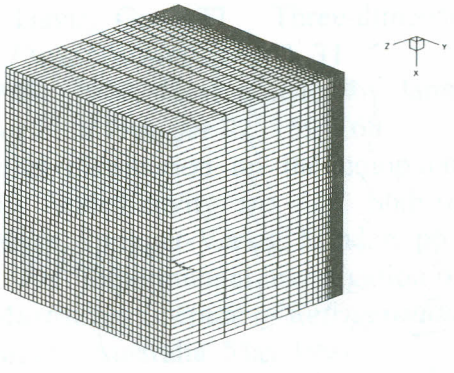

(a)

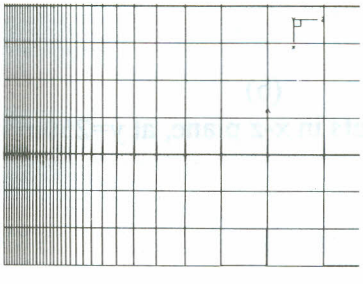

(b)

Figure 5. (a) View of the mesh distribution used in the computation and (b) near wall mesh resolution in the x-z plane.

CONCLUSION

An efficiency procedure for the mesh generation has been developed by the use of a grid generating function, which results in a strong grid refinement along the walls. Its efficient was illustrated by applying it to the problem of turbulent natural convection in an enclosure with colliding boundary layers. The essential feature of the procedure is the use of the exponent p, which has the effect of increasing the number of nodes away from the wall at which R_{max} occurs until, in the limit $p \rightarrow \infty^+$, R_{max} occurs at the last node I_c.

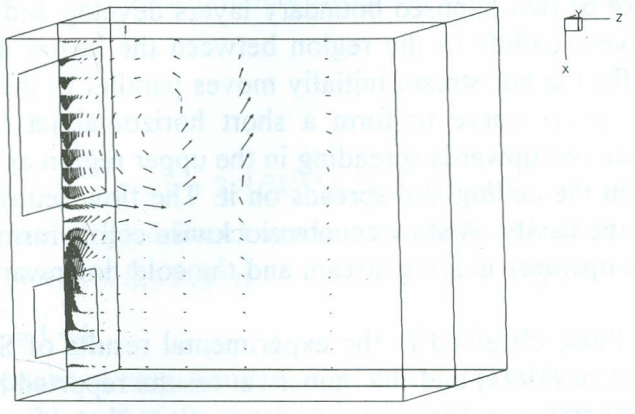

(a)

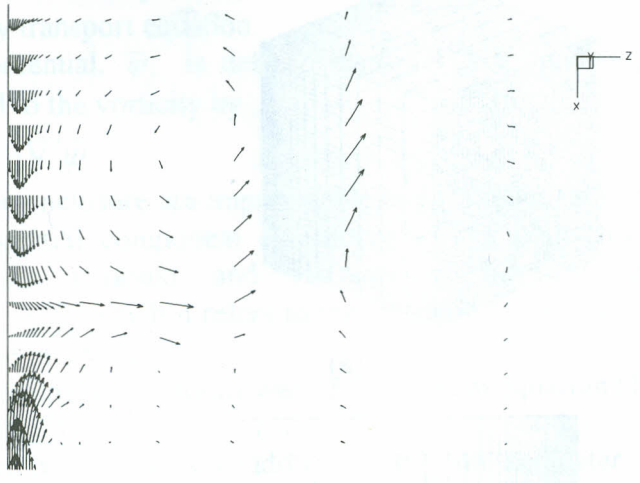

(b)

Figure 6. (a) Velocity vector plots in x-z plane, at y=250mm (b) side elevation.

REFERENCES

Cooper, P. and Kulkarni, R. 1993. Natural convection in an enclosure with colliding boundary layers: Experimental study. *Fifth Australasian Heat and Mass Transfer*, University of Queensland, Brisbane, Australia, August 1993, pp 69.1– 69.6.

Daly, B.J. and Harlow, F.H. 1970. Transport equations in turbulence. *The Physics of Fluids* 13: 2634–2638.

De Vahl Davis, G. Leonardi, E. and Wong, S.A. 1988. Three-dimensional natural convection in a room. *Second Australian Natural Convection Workshop.* University of New South Wales, Sydney, Australia, *Report 1988/FMT/5*, July 1988.

Gatheri, F.K., 1994. *Numerical simulation of turbulent natural convection in an enclosure*. Ph.D. Thesis, University of New South Wales, Sydney, Australia.

Hirasaki, G.J. and Hellums, J.D. 1968. A general formulation of the boundary conditions on the vector potential in three-dimensional hydrodynamics. *Quarterly of Applied Mathematics*, XXV: 331–342.

Humphrey, J.A.C. and Bleinc, C. 1985. On the structure of the flow, due to the collision of opposed vertical, free convection boundary layers. *International Communications in Heat and Mass Transfer* 12: 233–240.

Ince, N.Z. and Launder, B. 1989. On the computation of buoyancy-driven turbulent flows in rectangular enclosure. *International Journal of Heat and Fluid Flow* 10: 110–117.

Jones, I.P. and Thompson, C.P. 1980. On the use of non-uniform grids in finite difference calculation. *Numerical Methods in Thermal Problems*, Pineridge Press, Swansen, pp 338–348.

Jones, W.P. and Launder, B.E. 1972. The prediction of laminarization with a two equation of turbulence. *International Journal of Heat and Mass Transfer* 15: 301–314.

Launder, B.E. and Sharma, B. 1974. Application of the energy-dissipation model of turbulence to the calculation of flow near a spinning disc. *Letters in Heat Transfer* 1: 131–138.

Mallison, G.D. 1974. *Natural convection in an enclosed cavities*. Ph.D. Thesis, University of New South Wales, Sydney, Australia.

Mallison, G.D. and de Vahl Davis, G. 1977. Three-dimensional convection in a box: A numerical study. *Journal of Fluid Mechanics* 83: 1–31.

Newel, M.E. and Schmidt, F.W. 1970. Heat transfer by laminar natural convection within rectangular cavity. *Journal of Heat Transfer* 92: 159–168.

Quon, C. 1983. Effects of grid distribution on the computation of high rayleigh number convection in a differentially heated cavity. *In:* T.M. Shih (ed.), *Numerical Properties and Methodologies in Heat Transfer*, Springer-Verlag, London, pp 261–281.

Sanjurjo, B.E. and Cooper, P. 1991. Experimental investigation of air movement in a room using a water-filled scale model. *Australian Institute of Refrigeration, Air Conditioning and Heating (AIRAH) Conference*, Melbourne, Australia, May 1991.

Thomas, R.W. 1970. *Finite difference computation of heat transfer by natural convection*. Ph.D. Thesis, University of New South Wales, Sydney, Australia.